Journal of GeoEngineering, Vol. 3, No. 3, pp. 113-119, December 2008

TENSILE CREEP BEHAVIOR OF A PVC COATED POLYESTER GEOGRID AT DIFFERENT TEMPERATURES

Chiwan Hsieh[1] and Yen-Chen Tseng[2]

ABSTRACT

This study investigates the tensile creep behavior of a PVC coated polyester geogrid at different temperatures. The ultimate tensile strength of the test geogrid is 128(MD)/115(CD) kN/m. The geogrid was fabricated using knitting and woven techniques. A series of tensile tests (ASTM D6637) and conventional long-term (ASTM D5262) creep tests were performed to evaluate the tensile strength, elongation at rupture and long-term creep strains of the geogrid. The test results indicated that the ultimate tensile strength of the PET geogrid linearly decreased as the test temperature increased up to 60°C. The tensile strength decreasing rate is about –0.33% per degree of Celsius. The elongation at break is about 11% for the tested conditions varied from 0°C to 60°C. The tensile strength and elongation at break for the 80°C test condition was inconsistent with the results from other test conditions. It is believed that the phenomenon of glass formation might have some effects on the engineering behavior of the test geogrid at around 80°C. The creep strain rate also increased as the test temperature was increased under same tensile load condition. Linear creep strain rates were observed from a series of conventional long-term test product creep tests. Under conditions with same creep tensile load or same percentage UTS tensile load under higher temperature conditions presented higher total creep strain and associated creep strain rate. The creep modulus decreased as the test temperature was increased. The creep strain rate increase could be up to 80% for temperature condition changes from 20°C to 40°C. The required rupture time linearly decreases as creep load increased on a log time scale. The decreasing rate of rupture time increases as test temperature increased.

Key words: Geogrid, temperature, tensile strength, creep.

1. INTRODUCTION

Geosynthetics provide many reinforcement engineering application functions, such as separation, drainage, filtration, reinforcement, liquid barrier, erosion control and protection. The tensile strength and durability properties, such as molecular weight and Carboxical end group, must be evaluated for design purposes. Tensile strength is the most important design property among these tests. The long-term design strength can be obtained by dividing the ultimate tensile strength with appropriate reduction factor in considering the creep, installation damage and chemical/biological degradation. One of the main design concerns for the long-term stability of geosynthetic reinforced soil structures is creep behavior prediction for the geosynthetics under design loads. The long term stresses and strains in the reinforcement should not exceed their corresponding allowable design values during the life of the structure.

Currently, ASTM D6637 determines the tensile properties of geogrids using the single rib or multi-rib tensile method. This is the most common test method for evaluating the ultimate tensile strength of geogrids. The state-of-practice design methods and standards usually incorporate a reduction factor for creep, along with reduction factors for other degradation mechanisms to obtain the long-term strength (FHWA 1993; Task Force 27 1989). The reduction factor for creep load is determined using unconfined creep tests with a minimum duration of 10,000 hours (Allen 1991; GRI-GG4 1991; ASTM D5262). It is general practice that geosynthetic creep data from these tests can only be extrapolated up to one order of time magnitude (*i.e.*, up to 10 years) (FHWA 1993; Jewell and Greenwood, 1988). Several accelerated creep tests were proposed and approved can be use to estimate the long term creep performance of geosynthetics. In these tests, a creep load is applied to the geosynthetics at elevated temperatures. The results from these tests can be shifted to extrapolate the creep behavior at the same load levels to longer time intervals using time-temperature superposition principles (ASTM D6992).

Currently, the 21°C test temperature is the most common condition referred to in ASTM and ISO standards. However, the average temperature varies depending upon location and season. The temperature effect on tensile creep behavior needs further investigation.

2. OBJECTIVES

This paper presents the tensile creep behavior of a PVC coated polyester geogrid at different temperatures evaluated using the tensile strength and conventional long-term creep testing methods. The results from this study were used to provide the tensile and creep behavior of polyester geogrids under different temperature conditions. This information can be used if the design temperature differs from the standard 21°C test temperature.

3. TEST MATERIALS

A PVC coated polyester geogrids provided from a local (Taiwan) manufacturer was used for this study. The ultimate tensile strength of the geogrid is 128(MD)/115(CD) kN/m. The test geogrid was manufactured using knitting and weaving proc-

---

Manuscript received August 8, 2008; revised October 28, 2008; accepted November 19, 2008.

[1] Professor (corresponding author), Department of Civil Engineering, National Pingtung University of Science and Technology, Taiwan (e-mail: cwh@mail.npust.edu.tw).

[2] Graduate Student, Department of Civil Engineering, National Pingtung University of Science and Technology, Taiwan (e-mail: pk819@yahoo.com.tw).

esses. The product was made from high tenacity, high molecular weight (> 25,000 g/mole), alkali tolerant (max. 30 carboxyl end group) fibers. The glass transition temperatures of these fibers were around 76°C. The typical polyester fiber double hump stress versus strain response was observed for the tested product. The general properties of the tested geogrid are shown in Table 1.

4. TEMPERATURE VARIATIONS

The average monthly temperatures in Taipei, Tokyo, Singapore, Paris, Sydney and New York from 1961 to 2000 are summarized in Fig. 1 (www.cwb.gov.tw). The highest and lowest average monthly temperatures occurred in July and January for the cities located in the northern hemisphere. However, a reverse phenomenon was observed for the city of Sydney, located in the southern hemisphere. The data shown in the figure indicated that the average air temperatures could vary during a year and the manner of variation depends on location. The difference between the highest and lowest average monthly temperature in New York was about 24.9°C. This difference was the greatest among the cities shown in the figure. On the other hand, the average monthly temperatures for Singapore varied throughout the year ranging from 25.7°C to 27.4°C.

The average monthly air and ground temperatures observed at the weather station at National Pingtung University of Science and Technology (NPUST) from 2006 to 2008 are summarized in Fig. 2. As shown in the figure, the monthly average daily highest and lowest temperatures were generally 4°C to 5°C different from the average daily temperature. In general, the ground temperatures and the average daily air temperature showed good correlation. The average monthly air temperature, average monthly surface ground (–5cm) and shallow depth (–50 cm) ground temperatures were quite similar from April to September. However, the shallow depth (–50 cm) ground temperature would be 2°C to 3°C above the air temperature in the winter season. The NPUST ground temperature would vary ± 5°C through the year. Based upon the information shown in the two figures, ground temperature could vary from location to location and season to season. The air temperature and shallow depth ground temperature were close in the summer season. However, the shallow depth ground temperature would be slightly higher than the average air temperature in the winter season. This variation was quite different based upon the location. Currently, the 21°C test temperature is the most common condition referred to in ASTM and ISO standards. However, the present temperature of the geogrid used for reinforcement applications will vary based upon the site location and season. Therefore, the temperature effect on tensile and creep behavior in the PET geogrid is discussed.

Table 1 Summary of the tested material engineering properties

Item		Test method	Test results
			Type 1
Material		–	PVC coated polyester geogrid
Nominal strength (kN/m)		–	100 × 100
Junction weaving method		–	Woven and knitted
No. of rib per width	M.D.	–	31.78
	X.D.		37.19
Rib width (mm)	M.D	–	11.31
	X.D.		11.68
Rib spacing (mm)	M.D	–	20.79
	X.D.		15.54
P.O.A. (%)		–	35.64
Mass per unit area (g/m^2)	w. PVC coating	ASTM D5261	793.96
M.D. tensile strength (kN/m)		ASTM D6637	122.46
M.D. elongation at break (%)			11.06
X.D. tensile strength (kN/m)		ASTM D6637	114.55
X.D. elongation at break (%)			13.02

5. TENSILE TESTS AT DIFFERENT TEMPERATURES

A series of tensile tests was conducted for the test PVC coated Polyester geogrid at different temperatures. The test temperatures varied from 0°C to 80°C. The ASTM D6637 method B, wide width tensile test, was used to perform the tensile tests.

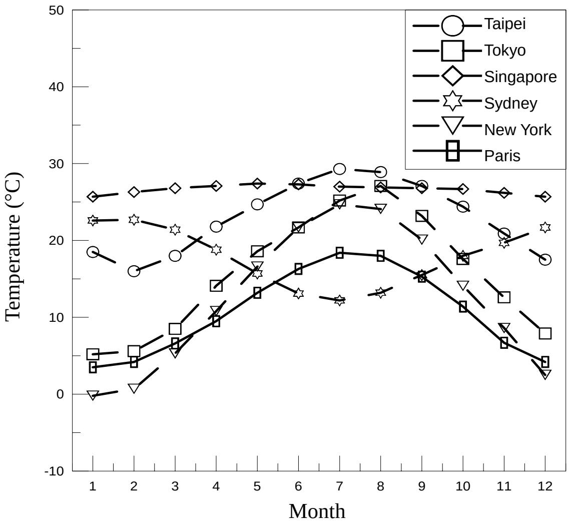

Fig. 1 Average monthly temperature for various cities

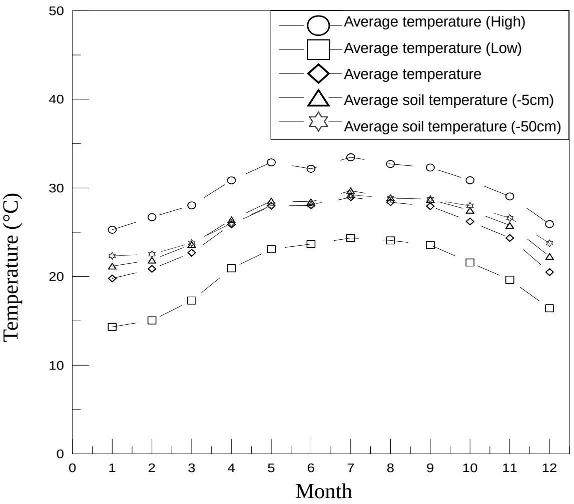

Fig. 2 Average monthly ground and air temperature at the National Pingtung University of Science and Technology weather station

The test specimen is 100 mm in width containing three longitudinal ribs. The test samples were conditioned in a constant temperature chamber with the test temperature for 24 hours before the test. Six test specimens were used for each tested temperature. The tensile test results for 20°C test condition are shown in Fig. 3. A typical double-S curve is observed. In addition, the test repeatability was quite good for all tested temperature conditions. The typical load versus elongation curves for different tested temperatures are shown in Fig. 4. The typical double-S curve was also observed for all tested temperature conditions. The elongation at break for the tested conditions, varied from 0°C to 60°C, were about 11% and quite similar to each other. However, the elongation at break at 80°C is about 10.25%. This value is significantly lower than the elongation at break values at other conditions. Generally, the ultimate tensile strength decreased as the test temperature increased. The ultimate tensile strength versus test temperature is further analyzed and plotted in Fig. 5. As shown in the figure, the ultimate tensile strengths decreased nearly linearly the test temperature decreased down to 60°C. The tensile strength decreasing rate is about –0.33% per degree of Celsius. The tensile strength and elongation at break for the 80°C test condition was inconsistent with the other test conditions. Because the glass transition temperature of PET yarn is near 80°C, the phenomenon of glass formation might have some effects on the engineering behavior of the test geogrid at around 80°C.

6. TENSILE CREEP TESTS AT DIFFERENT TEMPERATURES

6.1 Test

The conventional creep tests (ASTM D5262) were conducted at temperatures of 10°C, 20°C, 40°C, 60% RH, and at various creep tensile loads. For the conventional creep tests, two single-station and one multi-station rigid double-lever action creep frames, providing a 20:1 and 10:1 mechanical advantage in the loading train were employed, respectively. Temperature control with an accuracy of ±1°C was achieved using an environmental chamber and temperature-controlled room. The grips used in the wide width creep tests were a custom roller grip design fabricated in-house. Extension measurements for the creep test were made using a LVDT clamped to the specimens. A multiple-purpose environmental chamber (29 × 30 × 97 cm) with insulated walls was constructed to enclose the 215-mm wide width specimens and grips. The environmental chamber housed two 900W electrical heaters to achieve temperature jumps of 6 to 10°C within 2 ~ 4 minutes and maintain a constant temperature ±1°C during creep loading. The temperature was controlled using a custom made digital temperature controller with fuzzy logic capabilities equipped with an electronic thermocouple. Thermocouples for temperature control and data acquisition were positioned close to the specimen. Two 1/4 HP motors and two 5 by 2.5 inch fans were used within the environmental chamber to enhance air circulation and promote uniform temperature.

Displacements between the reference points in the specimen were measured using an external LVDT (Gefran Model PA1-F-100-S01M). The LVDT was directly mounted on the specimen with a gauge length of 100 mm. Because the LVDT measurements are temperature sensitive, temperature corrections were applied to the displacement data.

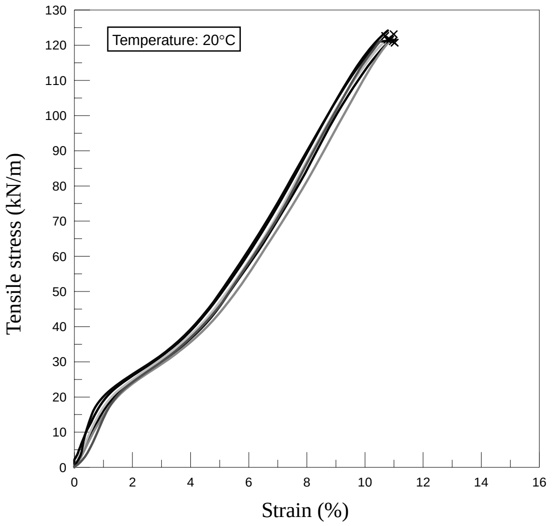

Fig. 3 Typical wide width tensile test results of longitudinal ribs for the geogrid at 20°C condition

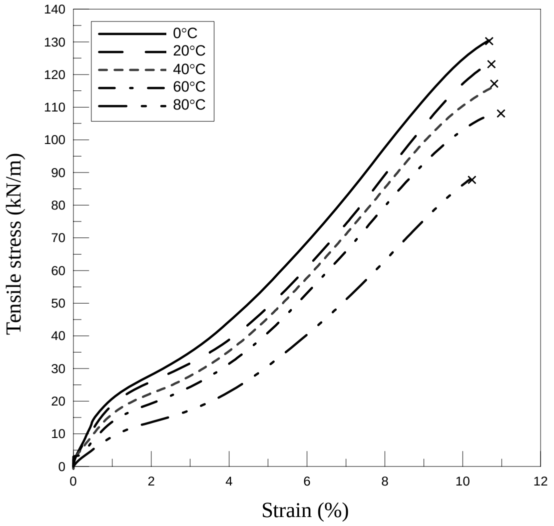

Fig. 4 Typical wide width tensile test results of longitudinal ribs of the test geogrid at various temperatures

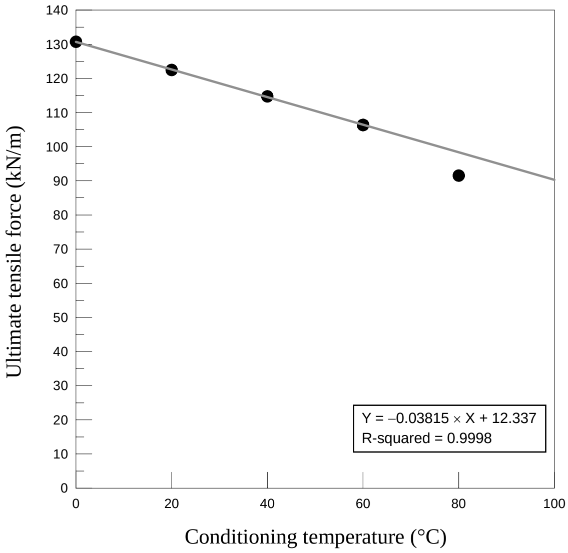

Fig. 5 Average tensile strength versus temperature for the test geogrid

Temperature, displacements and tensile load were recorded using an automatic data acquisition system. Data were collected every second to adequately capture the stress-strain response until rupture.

All tests were conducted using specimens from the same roll and performed using the same load frame, instrumentation, specimen preparation procedures and initial loading procedures. Testing was conducted in the machine direction (MD) of the geogrid specimens. Since wide specimens (100 mm or 200 mm in width as required) were used through-out the testing program, the test sampling and conditioning procedures were always conducted in general agreement with the wide-width (method B) tensile testing standard ASTM D6637 (ASTM 2003). A preload of 222 N or 1.25% of UTS (whichever lower) was applied prior to each test to condition the specimen and minimized the initial "setting in" of the stress-strain curve. The LVDT was mounted directly on the specimen upon preload completion.

6.2 Creep Strain

Greenwood (2004) noted that there can be quite a wide variability in the initial strain measurements for geogrids in creep tests. Therefore, a series of ramp and hold (R and H) short term creep tests was performed to determine the average short term elastic (creep) strain and modulus of the test geogrids. The R and H short term initial elastic (creep) strains and moduli results under 65% UTS tensile load at 10°C, 20°C and 40°C temperatures are summarized in Table 2. The initial elastic moduli were 1104, 1050, 989 kN/m for the test geogrid at test temperatures of 10°C, 20°C and 40°C, respectively. The initial elastic modulus decreased as the test temperature increased. The initial elastic (creep) modulus was used to adjust the long term creep curves for the test results.

As shown in Fig. 4, the ultimate tensile strength (UTS) of the test geogrid decreased as the test temperature increased. Therefore, the applied creep tensile load associated with a certain percentage of ultimate tensile strength would vary at different test temperatures. Therefore, the creep tensile load can be presented in the form of accurate load or percentage of UTS. Figure 6 shows the creep strain curves derived from 1000-hour conventional long-term creep test results for the test geogrid under same applied load (74.47 kN/m) at 10°C, 20°C and 40°C test temperatures. The creep loads were 59% UTS, 61% UTS, and 65% UTS for the associated temperature of 10°C, 20°C and 40°C, respectively. Generally, consistent linear creep strain is shown in log time scale. Please note that the curve associated with 40°C test condition showed higher initial elastic strain and creep strain than those for 10°C and 20°C conditions. However, the two creep curves seem parallel to each other up to 100 hours. The creep strain associated with 40°C test condition increases slight more than that for 20°C test condition after 100 hours.

Table 2 Summary of ramp and hold test results at various temperatures

No.	10°C		20°C		40°C	
	Strain (%)	Modulus (kN/m)	Strain (%)	Modulus (kN/m)	Strain (%)	Modulus (kN/m)
1	7.44	1121.62	7.68	1036.50	7.57	985.67
2	7.55	1105.28	7.53	1057.15	7.61	980.49
3	7.69	1085.15	7.54	1055.75	7.62	979.20
Average	7.56	1104.16	7.58	1049.59	7.60	981.47

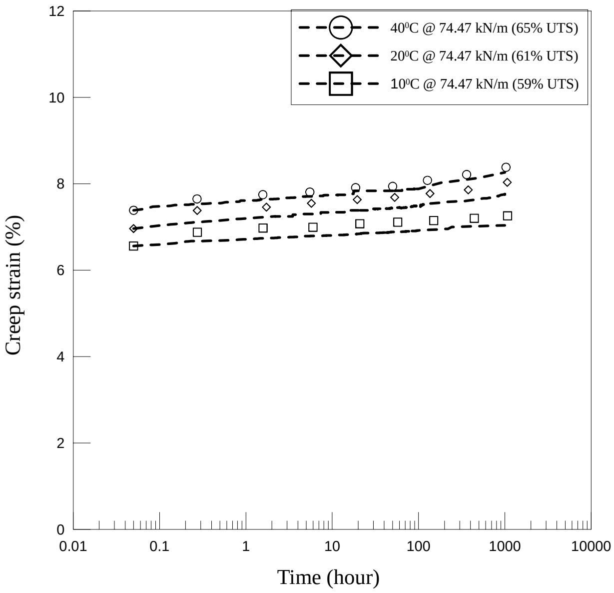

Fig. 6 Long term creep curves for 74.47 kN/m tensile load at 10°C, 20°C and 40°C

The load and strain data can be converted into the creep modulus for the tensile creep test. Figure 7 shows the analyzed creep modulus curves associated with the creep tensile test data shown in Fig. 6. The 1000-hour conventional long-term creep strains for the test geogrid at 10°C, 20°C and 40°C were 0.54%, 0.93% and 1.66%, respectively. As shown in the figure, the creep modulus linear decreases as increasing test duration on a log time scale. However, the creep modulus decreases as the test temperature increased. The reduction rate was about 14% for condition changes from 20°C to 40°C.

The associated creep strain rate curves showed in Fig. 8. The creep strain rate associated with the 40°C and 65% UTS load condition seems higher than that for that for the 20°C with 61% UTS and 10°C with 59% UTS load conditions. The creep strain rates decrease very rapidly at the initial stage and turn to plateau creep stage after 10 hours loading during the tests. As shown in the figure, secondary creep behavior was observed for both 1000-hour creep tests. Under conditions using the same creep tensile load, a higher condition temperature would present higher total creep strain and associated creep strain rate. The total creep strain increased near 80% under the same tensile creep load for the temperature condition change from 20°C to 40°C.

As discussed earlier, the ultimate tensile strength could vary for different test temperature. The 1000-hour creep tensile curves with 65% UTS tensile load at 10°C, 20°C and 40°C are showed in Fig. 9. The associated creep tensile loads are 84.64 kN/m, 79.56 kN/m and 74.47 kN/m, for temperatures at 10°C, 20°C and 40°C, respectively. Because the temperature effect on the initial creep strain slightly increases as the test temperature increases, these three creep curves are parallel to each other. The total creep strain increased as the test temperature increased. The 1000-hour conventional long-term creep strains for the test geogrid under 65% UTS tensile creep load at 10°C, 20°C and 40°C were 1.17%, 1.28% and 1.66%, respectively. The difference in creep strain could be up to 40% for temperature changes from 10°C to 40°C. Similarly, the creep modulus linear decreases as increasing test duration on a log time scale showed in Fig. 10. The creep moduli also decreased as the test temperature increased for the three test conditions.

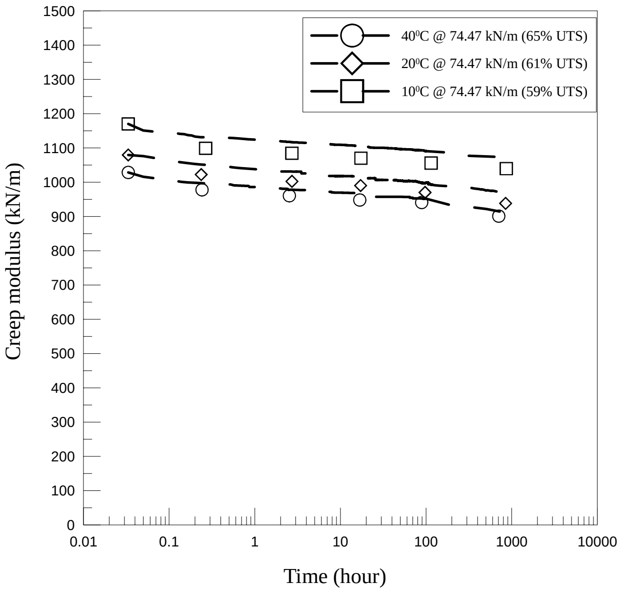

Fig. 7 Creep modulus versus time curves for 75.03 kN/m tensile load at 10°C, 20°C and 40°C

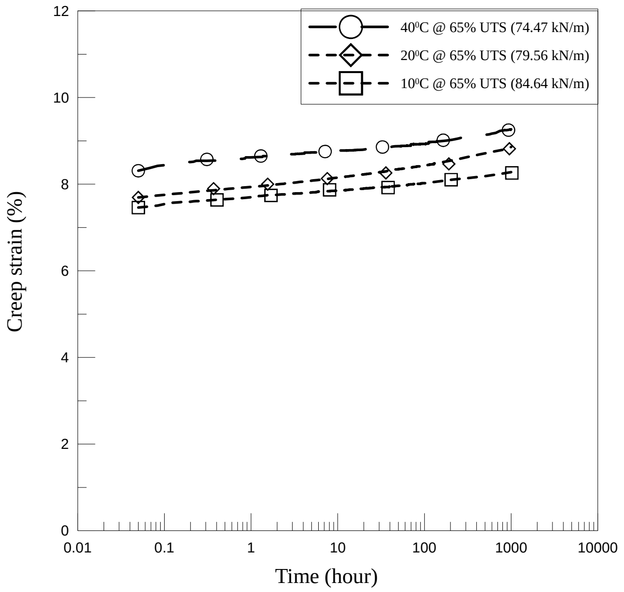

Fig. 9 Long term creep curves under 65% UTS loading at various test temperatures

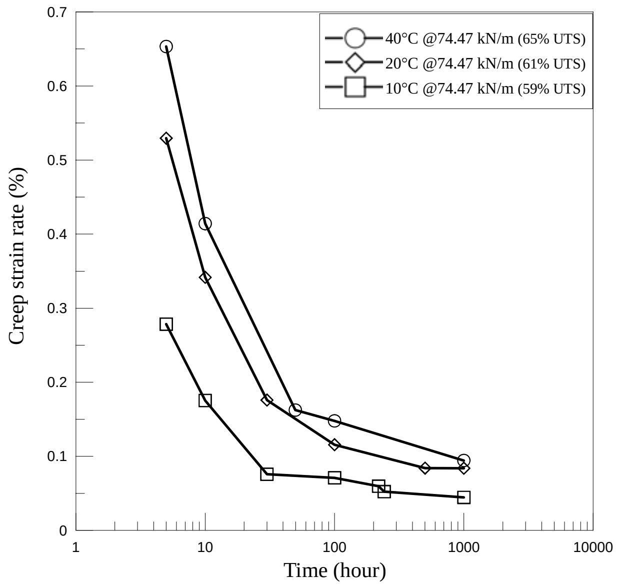

Fig. 8 Creep strain rate curves for 74.47 kN/m tensile load at 10°C, 20°C and 40°C

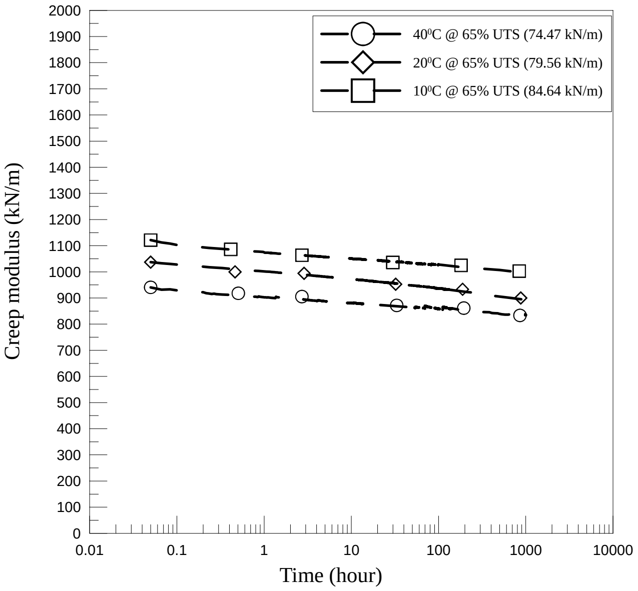

Fig. 10 Creep modulus curves under 65% UTS loading at various test temperatures

The associated creep strain rate curves for these three different test temperatures with 65 UTS load condition are shown in Fig. 11. The creep strain rate generally increases as the test temperature increased. As shown in the figure, the test condition with lower temperature will turn to plateau creep stage for less time duration. Secondary creep behavior was observed at 1000- hour duration for these three creep tests.

7. CREEP RUPTURE

Figure 12 presents the linear regression plots of rupture load as percentage of UTS versus log time to rupture for the conventional creep tests performed for temperatures at 10°C, 20°C and 40°C. These data points are located scatter around the regress lines for these test temperatures. As shown in the figure, the percentage of rupture load linear decreases as increasing test duration on a log time scale. The decreasing rate of creep rupture load increases as test temperature increased. Because of these behaviors, the long-term performance rupture load would decrease as test temperature increased. Therefore, it is important to know the design temperature in order to select adequate design factors during design stage.

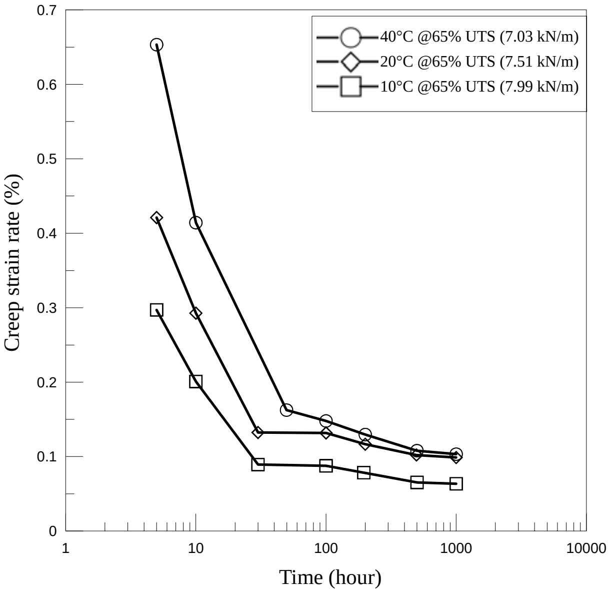

Fig. 11 **Creep strain rates under 65% UTS loading at various test temperatures**

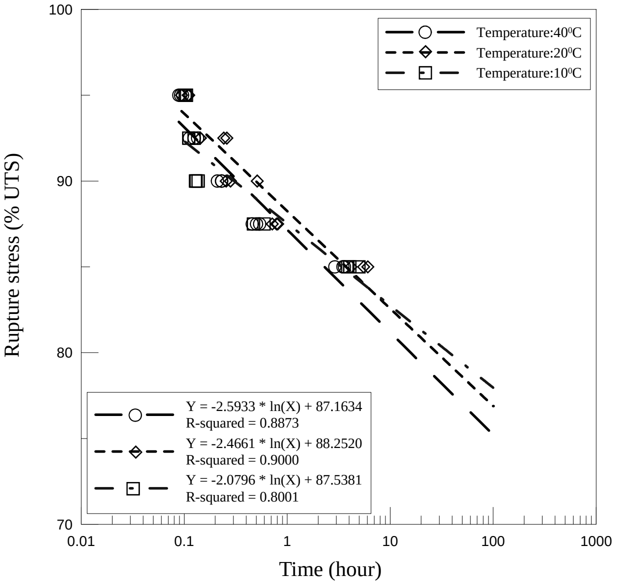

Fig. 12 **Creep rupture data and regression lines at various test temperatures**

8. SUMMARY AND CONCLUSIONS

The average air and ground temperatures vary from location to location and season to season. In addition, the air temperature and shallow depth ground temperature were found to be near or slightly different throughout the year. Therefore, the effect of temperature on the tensile creep behavior of PET geogrid was discussed in the paper. A PVC coated polyester geogrids provided from local (Taiwan) manufacturer was used in this study. The ultimate tensile strength of the geogrid at standard test condition is 128(MD)/115(CD) kN/m. A series of tensile tests was conducted for the test PVC coated Polyester geogrid at different temperatures. The test temperatures varied from 0°C to 80°C. ASTM D6637 method A was used to perform the tensile tests. The testing program also conducted a series of conventional creep tests (ASTM D5262) with 65% UTS creep tensile load at 10°C, 20°C, 40°C and 60% RH test conditions.

The ultimate tensile strengths (UTS) decreased linearly as the test temperature decreased. The decreasing rate is about –0.33% per degree of Celsius. The elongation at break for the tested conditions varied from 0°C to 60°C at about 11%. However, the tensile strength decreasing rate from 60°C to 80°C is slightly higher. The elongation at break for the 80°C condition was about 10.25%. Because the glass transition temperature of the test PET yarn is near 80°C, it is believed that the phenomenon of glass formation might have some effects on the engineering behavior of the test geogrid at around 80°C.

The initial creep strain from the creep tests can exhibit quite a wide variability. Therefore, a series of ramp and hold (R and H) short term creep tests at 59%, 61% to 65% UTS and different temperatures were performed to determine the average short term elastic strain and modulus of the tested geogrid. The initial elastic moduli of the tested geogrid were 1104.16, 1049.59, 989.47 kN/m at 10°C, 20°C and 40°C, respectively.

Linear creep strain rates were observed from a series conventional long-term creep tests on the tested product. In the condition with same creep tensile load, higher condition temperature presented higher total creep strain and associated creep strain rate. The difference in creep strain could be up to 40% for temperature changes from 10°C to 40°C. The creep strain rate increased near 80% for temperature condition changes from 20°C to 40°C. However, the creep modulus decreased as the test temperature was increased. The test condition with lower temperature will turn to plateau creep stage for less time duration. Secondary creep behavior was observed for both 1000-hour creep tests.

The required rupture time for different creep load linear decreases as creep load increased on a log time scale. The decreasing rate of rupture time increases as test temperature increased. Because of these factors, the long-term rupture load would decrease as test temperature increased. Therefore, the average temperature of the project site is an important factor for the project in the design stage.

ACKNOWLEDGEMENTS

The authors are indebted to Dr. Robert M. Koerner, Dr. George Koerner, and Y. Grace Hsuan for their helpful suggestions at GSI. Seven State Enterprise Co., Ltd. is also acknowledged for providing test material for the study.

REFERENCES

Allen, T. M. (1991). “Determination of the long term tensile strength of geosynthetics; a state of-the-art review.” *Proceedings of Geosynthetics ’91 Conference*, Atlanta, 351–379.

ASTM D6637, (2003). “Standard test method for determining tensile properties of geogrids by the single or multi-rib tensile method.” *American Society for Testing and Materials*, West Conshohocken, PA.

ASTM D5262, (2002). “Standard test method for evaluating the unconfined tension creep behavior of geosynthetics.” *American Society for Testing and Materials*, West Conshohocken, PA.

ASTM D6992, (2003). "Standard method for accelerated tensile creep and creep-rupture of geosynthetic materials based on time-temperature superposition using the stepped isothermal method." *American Society for Testing and Materials*, West Conshohocken, PA.

Bush, D. I. (1990). "Variation of long-term design strength of geosynthetics in temperatures up to 40°C." *Proceedings, 4th International Conference on Geotextiles, Geomembranes, and Related Products*, 673–676.

FHWA, (1993). *Guidelines for Design, Specifications, and Contracting of Geosynthetic Mechanically Stabilized Earth Slopes on Firm Foundations*. FHWA-SA-93-025.

Farrag, K. and Shirazi, H. (1997). "Development of an accelerated creep testing procedure for geosynthetics—Part I: Testing." *ASTM Geotechnical Testing Journal*, **20**(4), 414–422.

Farrag, K. (1998). "Development of an accelerated creep testing procedure for geosynthetics—Part II: Analysis." *ASTM Geotechnical Testing Journal*, **21**(1), 38–44.

Greenwood, J. H., Kempton, G. T., Brady, K. C. and Watts, G. R. (2004). "Comparison between stepped isothermal method and long-term creep tests on geosynthetics." *Proceeding, 3rd European Geosynthetics Conference*, Munich, Germany, 527–532.

GRI-GG4 Standard Practice, (1991). "Determination of the long term design strength of stiff geogrids." *Geosynthetics Research Institute*, Drexel University.

Jewell, R. A. and Greenwood, J. H. (1988). "Long term strength and safety in steep soil slopes reinforced by polymer materials." *Geotextiles and Geomembranes*, No. 7, 8–118.

Task Force No. 27, (1989). "Design guidelines for use of extensible reinforcements (geosynthetic) for the mechanically stabilized earth walls in permanent applications." *Joint Committee of AASHTO-AGC-ARBTA on Materials*.

Thornton, J. S., Paulson, J. N. and Sandi, D. (1998). "Conventional and stepped isothermal methods for charactering long term creep strength of polyester geogrids." *Proceedings, 6th International Conference on Geosynthetics*, Atlanta, 691–698.

Thornton, J. S., Sprague, C. J., Klompmaker, J. and Weeding, D. B. (1999). "The relationship of creep curves to rapid loading stress-strain curves for polyester geogrids." *Proceedings, Geosynthetics '99*, 735–744.

Wrigley, N. E., Wei, L. and Junyi, P. (2004). "Accelerated creep testing and quality assurance." *Proceeding of 3rd European Geosynthetics Conference*, Munich, Germany, 551–556.

Yeo, K. C. (1985). *The Behavior of Polymeric Grids Used for Reinforcement*. Ph.D. Dissertatiion, University of Strathclyde, Glasgow, U.K.

Zornberg, G. G., Byler, B. R. and Knudsen, J. W. (2004). "Creep of geotextiles using time-temperature superposition methods." *Journal of Geotechnical and Geoenvironmental Engineering*, ASCE, **130**(11), 1158–1168.